3D EXPLOITATION OF SATELLITE IMAGES FOR DEM GENERATION

Iulia DANA, Research assistant – Romanian Space Agency, iulia.dana@rosa.ro
Florea ZAVOIANU, Prof. Dr. Eng. – Faculty of Geodesy, Technical University of Civil Engineering Bucharest, florea.zavoianu@gmail.com

***Abstract**: This paper presents two different techniques for generation of Digital Elevation Models (DEMs): stereoscopy using optical satellite images (SPOT 5 HRG data) and interferometry using Synthetic Aperture Radar (SAR) images (ERS 1/ERS 2 Tandem, ENVISAT ASAR, TerraSAR-X StripMap and High Resolution Spotlight data). In the framework of the case study, two test sites have been selected: Bucharest (urban area) and Siret (flat up to rolling area, located in the Siret Basin). In case of test area Bucharest, a number of Digital Surface Models (DSMs) have been generated by means of automatic image matching and interferometry using the above mentioned satellite data. For test area Siret, the DSM have been generated using only optical stereoscopy. This model have been filtered in order to remove the points that don't belong to the bare ground and to obtain the DEM.*

***Keywords:** digital surface model, digital elevation model, interferometry, stereoscopy.*

1. Introduction

A digital elevation model (DEM) consists of a number of points with X, Y and Z coordinates describing the bare soil. The generation of DEMs based on remotely sensed data can be efficient and cost effective. Basically, the methods used for DEM generation can be divided in two main categories: (1) stereogrammetry techniques, using aerial/satellite imagery or radar data, and (2) radar interferometry [1]. Initially, DEMs are digital surface models (DSM) containing points located on top of the visible surface, including buildings and vegetation. These DSMs have to be filtered in order to remove all the points that do not belong to the bare ground [2] and to obtain the final DEM. DEMs are currently used in a wide range of scientific, commercial, industrial, and military applications.

At global level, the lack of qualitative and available DEMs has been covered by the Shuttle Radar Topography Mission (SRTM) launched in February 2000, having a SAR (Synthetic Aperture Radar) sensor on board. This model includes the continental regions located between 56^0 south latitude and 60.25^0 north latitude and it has a spatial resolution of 3 arc seconds ≈ 90 m (available free on the Internet) or 1 arc seconds ≈ 30 m (fee). Presently, at 30 m resolution, there are ASTER Global DEM (free dataset) with a 99% coverage at global level and SPOT 3D model (fee), generated based on the satellite images acquired by the HRS sensor. At national level, the National Agency for Cadastre and Land Registration (NACLR) has produced digital elevation models with a grid spacing of 2 m, 3 m, 6 m, 10 m, 15 m, 20 m or 30 m. Unfortunately, these models are not available for every region of the Romanian territory, each at spatial resolution mentioned above.

The main objective of this study is represented by the generation of the digital surface models (DSMs) based on the data acquired by passive and active remote sensing sensors and the comparison of the results obtained after data processing. Using SPOT 3D as reference model, the accuracy of these DSMs was analyzed. Also, for one of the selected test sites, the filtering of the generated DSMs has been performed and the resulting DEMs were analyzed.

2. Test areas

The first test area is represented by the city of Bucharest. The DSMs analysis was performed over a subset test area of 5 km x 4 km that has the House of the Parliament in the center. The coordinates of this subset test are: 425000 E, 4922000 N [m] for the upper left point and 430000 E, 4918000 N [m] for the lower right point, 430000 E, 4918000 N [m], UTM (Universal Transverse Mercator) projection, zone 35^0N, WGS84 (World Geodetic System) ellipsoid. According to the digital surface model considered as reference model (SPOT 3D), the height within the test area ranges between 97 m and 155 m. This built-up area is characterized by the usual urban complex pattern: mixture of buildings with different height levels, paved roads, vegetation, and water bodies.

The second test area is located in the Lower Siret Basin and it is covering territories from four different counties: Galati, Vrancea, Bacau, and Vaslui. The size of this area is 6.5 km x 14.5 km, whereas the heights are between 73 m and 301 m. The coordinates of this test area in UTM projection, zone 35N, WGS84 ellipsoid are: 530500 E, 5113500 N for the upper left point and 537000 E, 5099000 N for the lower right point. This flat up to rolling area basically consists of small villages, pastures, agricultural fields, and forests.

3. Methodology

Optical stereoscopy consists of all the principles and laws that govern the binocular view, as well as the means of obtaining it. In case of binocular view, the spatial image appears at brain level through the fusion of two different images formed simultaneously by the eyes [3]. The parameters that should be considered when choosing a couple of stereoscopic images are: the base-to-height ratio, the time interval between the acquisition of the two images and the percent of overlap between the two images.

The first step in DSM generation using optical stereoscopy is represented by the selection and measurement of the control points (CP) needed for image orientation and of the tie points used in the automatic image matching process. At pixel level, the inherent parallaxes between the two stereoscopic images are measured. The values of the parallaxes are transformed in absolute height by means of automatic image matching based on the control and tie points. The computation of the heights is executed for every pixel of the stereo-model, next step consisting of the projection of these points into the ground coordinate system. The result of the automatic image matching is represented by the digital surface model. This model contains certain areas in which the corresponding points could not been identified in both images during the process of automatic image matching. Therefore, for these image areas, the height of the points could not be determined, their most likely values being calculated using interpolation.

The accuracy of a digital surface model is estimated against a reference digital surface model, by computing the root mean square error RMSZ (1) and the standard deviation σ_Z (2), where *n* represents the number of points and *ME* represents the average:

$$RMSZ = \sqrt{\frac{\Sigma\left(Z_{DSM} - Z_{REF}\right)^2}{n}} \qquad (1)$$

$$\sigma_Z = \sqrt{\frac{\Sigma\left[\left(Z_{DSM} - Z_{REF}\right) - ME\right]^2}{n-1}} \tag{2}$$

Interferometry consists in the use of the phase of a radar signal by comparing two radar images acquired simultaneously or in a certain time interval [4]. The selection criteria for interferometric pairs are based on the following elements: the angle and direction of acquisition, the geometric and temporal baseline, the moment of acquisition, the coherence and the atmospheric conditions.

In the first step, the interferometric processing implies the registration of the images, considering the orbital inaccuracies, the different altitudes of the acquisition sensors and the re-sampling coefficients for each image [5]. Next, the synthetic interferogram is generated based on the orbital parameters and the information concerning the topography of the terrain. Using the baseline information and the orbital parameters, the interferogram is computed by combining the two images and generating the interferometric fringes [5]. Usually, in the case of the interferograms generated based on radar images acquired over large time intervals, the phenomenon of time decorrelation appears, that is translated in an interferometric phase affected by noise. Noise reduction is done by averaging the neighbored pixels of the complex interferogram [5], [6]. Phase noise can be estimated by computing the local coherence coefficient. The differential interferogram is calculated by removing the influence of the terrain topography using the parameters of a reference ellipsoid or a DEM [5]. Next, phase unwrapping is performed, by retrieving the integer number of cycles that is added to the unwrapped phase, so the absolute phase could be obtained for each and every pixel. The last step of the processing chain is represented by absolute interferometric phase conversion into height and DSM creation [5]. The standard deviation of the heights of the DSM points is determined using formula (3), where care γ represents the local coherence, N is the interferogram multi-looking factor, B is the perpendicular baseline, R is the sensor-target distance, θ is the incidence angle and λ is the wavelength of the radar signal:

$$\sigma_h = \sqrt{\frac{1-\gamma^2}{2\gamma N}} \frac{R\lambda \sin\theta}{4\pi B} \tag{3}$$

4. Input data

The characteristics of the satellite images used in the framework of the study are presented in Table 1 (passive remote sensing sensor) and Table 2 (active remote sensing sensors). The SPOT 5 HRG stereoscopic images for test area Bucharest were acquired one day apart from each other and they are almost completely overlapping. Regarding the SPOT 5 HRG stereo-couple for the second test area (Siret), the time interval for acquisition is one week, and the overlapping percent is much lower, approximately 18% from the entire image. All SPOT 5 HRG images used in this study have 5 m spatial resolution (panchromatic). ERS images were acquired during the Tandem mission, while the ENVISAT ASAR I2 images present a time interval of 735 days between the two acquisitions. Both ERS and ENVISAT data are from track 465 (VV polarization). TerraSAR-X data were acquired from an ascending orbit, track 9, having HH polarization. In case of TerraSAR-X StripMap (TSX SM) images the range bandwidth is 100 MHz and the resolution is 1.8 m (slant range) x 3.0 m (azimuth). TerraSAR-X High Resolution Spotlight (TSX HS) images were acquired using a range bandwidth of 300 MHz. TSX HS images have 0.6 m resolution in slant range and 1.1 m resolution in azimuth. Reference data consists of the SPOT 3D model (30 m resolution at the equator); all the generated DSMs were analyzed against this model. Also, the SRTM (3 arc seconds resolution at the equator) model have been included into the final comparative analysis of the results.

Table 1. Characteristics of the SPOT 5 HRG stereoscopic data

Sensor	Date	Orbit	Incidence angle	Base-to-height ratio	Overlapping area [km]
SPOT 5 HRG Bucharest	29.08.2005	092-260	23.8^0	0.51	58 x 60
	30.08.2005	092-260	4.2^0		
SPOT 5 HRG Siret	15.05.2007	094-257	28.3^0	0.98	15 x 44
	22.05.2007	093-257	23.9^0		

Table 2. Characteristics of the ERS, ENVISAT and TerraSAR-X interferometric data

Sensor	Date	Orbit	Incidence angle	Perpendicular baseline [m]	Height of ambiguity [m]
ERS Tandem	08.10.1999	465	23.3^0	228.90	42.01
	09.10.1999	465	23.3^0		
ENVISAT ASAR	11.03.2006	465	22.8^0	153.29	61.38
	15.03.2006	465	22.8^0		
TerraSAR-X SM	12.02.2008	9	41.1^0	55.49	125.09
	27.03.2008	9	41.1^0		
TerraSAR-X HS	30.09.2008	9	41.4^0	45.75	143.52
	11.10.2008	9	41.4^0		

The base-to-height ratio is calculated based on the incidence angles of the two stereoscopic images. For SPOT HRG stereo-couples, the base-to-height ratio ranges between 0.50 and 0.80. If the terrain is hilly the base-to-height ratio must be low (0.50), but if the terrain is flat a base-to-height of 0.80 is better. Also, values close to 1 are accepted for this parameter. For Synthetic Aperture Radar (SAR) data, the height of ambiguity is defined as the altitude difference that generates an interferometric phase change of 2π and it is inversely proportional to the perpendicular baseline [5]. The height of ambiguity was calculated for each interferometric pair using the wavelength of the carrier wave, the range of the target, the look angle and the perpendicular baseline.

Both for the optical and radar data, the (x, y) coordinates of the control points were extracted from the digital orthophotos (0.5m spatial resolution), Stereographic '70 Projection, Pulkovo 1942 datum, Krassovski 1940 ellipsoid. These coordinates were transformed from the Stereographic '70 Projection into the CRS ETRS89 system (Coordinate Reference System - European Terrestrial Reference System), GRS80 ellipsoid. The CRS ETRS89 coordinates, ellipsoid GRS80 were considered to be identical with the geographic coordinates, WGS84 datum, and WGS84 ellipsoid. Next, these coordinates were transformed into UTM projection system, zone 35^0N, WGS84 datum, and WGS84 ellipsoid. For the Z coordinate, a change of the SPOT 3D DSM vertical datum was performed from EGM96 (World Wide 15-Minute Geoid Height) to WGS84. That means that the orthometric heights (EGM96 datum) were transformed into ellipsoidal heights (WGS84 datum).

5. Results

5.1. Generation of DSMs

Optical stereoscopy – for test area Bucharest, the georeferencing of the SPOT 5 HRG images (5 m spatial resolution) was performed using the indirect method that is based on the control points. For this purpose, 90 control points were measured. The mathematic model of the transformation is represented by the rational polynomials. Based on the residual errors, the root mean square error was estimated for each axis: ± 18.11 m ≈ ± 3.6 pixels for X axis, ±16.07 m ≈ ±3.2 pixels for Y axis and ±14.50 m for Z axis.

The stereo-model was created using automatic imaging matching by identifying the corresponding points in the two images, thus being used 10 tie points and the residual Y parallax having a value of ± 0.5826 pixels (or ± 2.9130 m). The accuracy of the relative image orientation, in relation to the residual parallax of the corresponding points, has the value of ± 1.705 m. This one-dimensional matching method that uses the epipolar lines implies the generation of the epipolar images. Identification of the corresponding points within the two images was executed through automatic image matching using a search window of 13x13 pixels and a threshold of 0.70 for the correlation coefficient.

The same processing chain was applied for the SPOT 5 HRG images that cover the second test area, namely Siret. Due to the fact that in this case the overlapping area is smaller, only 15 control points were used for georeferencing. The root mean square errors are: ± 4.57 m ≈ ± 0.9 pixels for X axis, ±9.08 m ≈ ±1.8 pixels for Y axis and ±18.34 m for Z axis. The residual Y parallax of ± 0.3548 pixels (or ± 1.7740 m) was determined based on 9 tie points that were uniformly distributed over the overlapping area. The overall accuracy of the relative image orientation has the value of ± 1.019 m. The automatic image matching was performed by setting a value of 0.70 for the correlation coefficient and a search window of 13x13 pixels.

In both cases (test area Bucharest and test area Siret), the result of the automatic image matching is represented by the digital surface model [5], UTM projection system, zone 35^{o} N, WGS84 ellipsoid, 15 m spatial resolution (a square network of points with 15 m spacing obtained by bilinear interpolation in order to remove the information gaps and to create a uniform distribution of the points contained by the surface).

Interferometry – the interferometric processing of ERS, ENVISAT and TerraSAR-X data has basically followed the same steps, with few exceptions. First, the application of precise orbits was possible only in the case of ENVISAT data (available on the ESA FTP site). For ERS Tandem images, the precise orbits were not available. TerraSAR-X data are extremely precise and do not require additional orbit files.

Next, the coarse and fine coregistration was performed by evaluation of the cross-correlation measurements based on the complex input data. For ERS Tandem data, image registration has been executed by using a grid of 289 tie points and a minimum threshold of 0.21 for the correlation coefficient. Also, 4 ground control points were measured for orbital corrections because there were no precise orbits available for both ERS Tandem images. Ground control points identification within SAR (Synthetic Aperture Radar) images is extremely difficult, especially in case of ERS and ENVISAT as a result of their lower resolution. Moreover, point identification is made in the slant range acquired images, therefore the image in mirrored along the vertical or horizontal axis and the distances are distorted. The overall residual error of the ground control points has the value of ± 0.5265 m (± 0.4155 m in azimuth and ± 0.3234 m in slant range). In case of ENVISAT, image registration was performed using 144 tie points, of which 100 have exceeded the threshold of 0.25 set for the correlation coefficient. Image registration for TerraSAR-X SM data was executed using a grid of 400 tie points, a 256 pixels reference window, a 144 pixels search window and a 0.20 minimum value for the correlation coefficient. In this phase, 4 control points were measured; these points have an overall residual error of ± 1.39 m (± 0.47 m in azimuth direction and ± 1.31 in slant range direction). The parameters used for the automatic registration of the TerraSAR-X HS images are: 0.30 threshold set for the correlation coefficient and a network of 380 tie points. The results of image registration are impressive because the images overlap perfectly, without the measurement of any ground control point. This fact is due to the very precise orbits and to the special image acquisition mode.

Within the coregistration phase, the slave image was resampled over the master image. The precision of coregistration is very important for the phase quality of the interferogram [4].

In the following step, the synthetic interferogram was generated based on the orbital parameters and the reference DSM (SPOT 3D); the resolution of the reference DSM is 22 m at the mean latitude of the test areas (30 m resolution at the equator). Then, the interferogram was calculated by cross multiplying, pixel by pixel, the first SAR image with the complex conjugate of the second [5]. The noise that affects the interferogram was reduced by averaging adjacent pixel in the complex interferogram using a multi-looking factor of 2x10 (2 looks in range, 10 looks in azimuth) for ERS and ENVISAT data, 12x12 in case of TSX SM and 20x20 for TSX HS data.

Interferogram filtering was executed next in order to improve the phase signal-to-noise ratio (SNR); a filter of 0.4 (where 0 represents no filtering and 1 maximum filtering) was applied using a window of 64 pixels. By subtracting the synthetic interferogram from the filtered interferogram, the differential interferogram was created.

Within a pixel, the difference in phase between two complex SAR images can be translated into a combination of contributing factors like topography, ground displacement, atmosphere and noise [7]. Coherence is a self-validating indicator of the phase measurement which depends on the proportion of useful signal to non-useful signal [4]. Thus, the phase noise can be estimated by means of the local coherence γ and it represents the cross-correlation coefficient of the SAR image pair estimated over a small window once all the deterministic phase components are compensated for [5]. After the generation and analysis of the coherence maps, the highest coherence values were obtained in case of TerraSAR-X data (0.44 average value) and the lowest in the case of ENVISAT data (0.14 average value). The coherence coefficient ranges between 0 and 0.92 with an average of 0.41, for ERS Tandem data. These high values were obtained due to the time interval of 1 day between the two image acquisitions, during which there were no significant changes in the landscape. The presence of coherence in the regions surrounding the urban area, in case of the agricultural fields, is remarkable. Usually, these areas lose coherence even in short time intervals, but in this case the coherence was kept also due to the 5.6 cm wavelength (C band) of the SAR sensor, which leads to a slower decorrelation in comparison with a 3 cm wavelength (X band). For ENVISAT, the coherence coefficient recorded values are between 0 and 0.89 with an average of 0.14. The average of the coherence coefficient values is much lower as a result of a very large time interval of approximately 700 days between acquisitions. The analysis of the coherence map shows that the only elements with higher coherence values are represented by built-up areas. The TerraSAR-X SM coherence map consists of coherence coefficient values that are in the range of 0 ÷ 0.99 with an average of 0.30. The highest values of the coherence coefficient were recorded in case of some greenhouses that were identified in the digital orthophotos first and then in the field. In case of TerraSAR-X SM, the coherence coefficient values are in the range of 0 and 0.99 and their average is 0.44.

Next, phase unwrapping was executed using the MCF (Minimum Cost Flow) algorithm, developed by the German Aerospace Center. Usually, the threshold set for the coherence coefficient is 0.65.

Geometry optimization was performed based on the ground control points measured in the registration step. Thus, the interferometric baseline was adjusted and the differential interferogram and the unwrapped phase were computed again. In case of ERS Tandem data, a correction of 56 cm has been applied to the initial baseline, the new value for the perpendicular baseline being 229.46 m. Similar, a correction of 26 cm was applied to the perpendicular baseline of the TerraSAR-X SM interferometric pair (new value: 55.23 m).

Next step consisted of the phase to height conversion; the generated DSMs are in UTM projection system, zone 35^0N, WGS84 datum, WGS84 ellipsoid (ellipsoidal heights). In order to fill in the gaps of information, the DSMs were interpolated (method: bilinear interpolation) using a regular grid with a spacing of 25 m for ERS and ENVISAT, 12 m for TSX SM (accordingly to the specifications of the future TanDEM-X Mission) and 5 m for TSX HS. The TSX HS resulting model presents with very high accuracy the terrain details. For example, within this model, the House of the Parliament has a realistic representation and can be easily identified. This level of detail has never been obtained in none of the previously presented cases. By overlapping the TerraSAR-X HS model over the orthophoto illustrating the city of Bucharest, a perfect alignment was noticed.

5.2. Editing and filtering of DSMs

The DSMs generated in the previous paragraph were edited for the purpose of removing their artifacts. For each DSM, an image containing the height difference between the analyzed model and the reference model (SPOT 3D) was generated. The values of this differential model that were not belonging to the normal distribution interval were replaced with values from the reference model. This operation was performed using band mathematics.

Next, a median filter was applied to each DSM in order to obtain a smooth surface. The median filter smoothes the surface and preserves the edges. Within a window, the value of each center pixel is replaced with the mean value of the neighbored pixels.

5.3. Comparative analysis of DSMs

Bucharest test area (illustrated in the colored orthophoto, copyright National Agency for Cadastre and Land Registration - NACLR) is presented in Fig. 1. The accuracy of the DSMs was analyzed against the SPOT 3D reference model (22 m pixel spacing) – Fig. 2. The analysis was executed using the "Analysis of digital elevation models" (DEMANAL) software, Program System BLUH, using two iterations. The DSMs used in the comparative analysis are presented in Fig. 3 - Fig. 7. In the comparative study, the SRTM DSM (71 m pixel spacing at the latitude of the test area) have been added (Fig. 8). Similar, for test area Siret (colored orthophoto, copyright NACLR – Fig. 9), the SPOT 5 HRG DSM was analyzed against the SPOT 3D model. These DSMs are presented in Fig. 10 and Fig. 11.

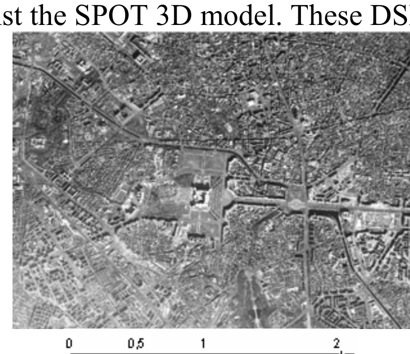

Fig. 1. Test area Bucharest (colored orthophoto © all rights reserved to NACLR)

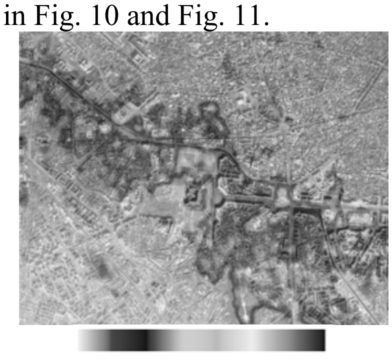

Fig. 2. SPOT 3D DSM (© SPOT IMAGE 2007) – 22 m resolution

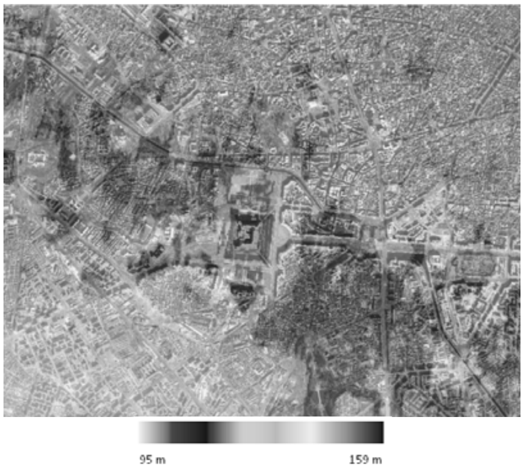

Fig. 3. SPOT HRG DSM - 15 m resolution, generated based on SPOT HRG data (© CNES 2009, distribution SPOT IMAGE S.A.)

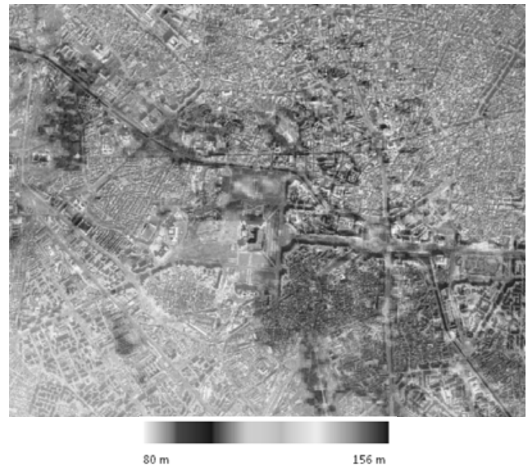

Fig. 4. ERS TANDEM DSM – 25 m resolution, generated based on ERS data (© ESA 2009)

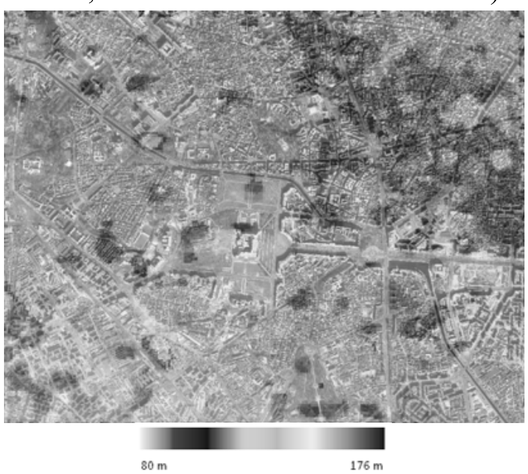

Fig. 5. ENVISAT DSM – 25 m resolution, generated from ENVISAT data (© ESA 2009)

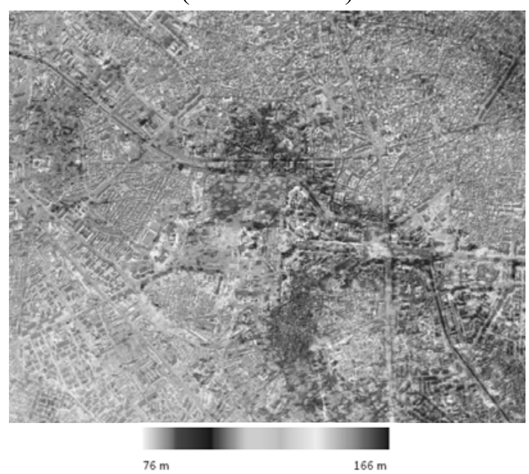

Fig. 6. TSX SM DSM - 12 m resolution, generated from TSX SM data (© DLR 2008)

Fig. 7. TSX HS DSM - 5 m resolution, generated from TSX HS data (© DLR 2008)

Fig. 8. SRTM DSM – 71 m resolution (© Jarvis A., H. Reuter, A. Nelson, E. Guevara*)

Fig. 9. Test area Siret (colored orthophoto © all rights reserved to NACLR)

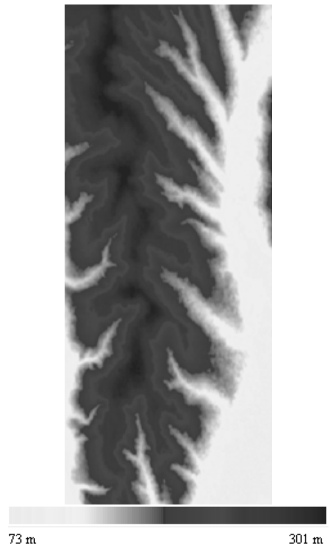

Fig. 10. SPOT 3D DSM (© SPOT IMAGE 2007) – 22 m resolution

Fig. 11. SPOT HRG DSM - 15 m resolution, generated based on SPOT HRG data

*© Jarvis A., H.I. Reuter, A. Nelson, E. Guevara, 2008, Hole-filled seamless SRTM data V4, International Centre for Tropical Agriculture, available from http://srtm.csi.cgiar.org.

The results of the comparative analysis of the DSMs generated for test are Bucharest are presented in Table 3. The results obtained for test area Siret are presented in Table 4.

Table 3. Results of DSMs analysis for test area Bucharest

DSM analysis	RMSZ [m]	Bias [m]	RMSZ without bias [m]
SPOT 3D – SPOT 5 HRG	3.46	-2.09	2.76
SPOT 3D – ERS TANDEM	4.75	-0.08	4.75
SPOT 3D – ENVISAT	7.93	-3.71	7.01
SPOT 3D – TSX SM	6.60	0.65	6.57
SPOT 3D – TSX HS	11.80	-1.15	11.74
SPOT 3D – SRTM	2.20	-0.18	2.19

Table 4. Results of DSMs analysis for test area Siret

DSM analysis	RMSZ [m]	Bias [m]	RMSZ without bias [m]
SPOT 3D – SPOT 5 HRG	4.27	-0.16	4.27

5.4 DEM generation

The filtering of the DSM implies the removal of the points that do not belong to the bare ground, and consequently the generation of the DEM. In the framework of the present study, DSM filtering was executed only for test area Siret, using the "Analysis and filtering of a DEM available in grids with equal spaces" (RASCOR) software. The filtering is possible by analyzing the minimal and maximal height in the area, the maximal height differences between neighbored points or the sudden change of the height level. For better filtering results, a forest mask layer have been added.

6. Conclusions

For test area Bucharest, the results of the comparative analysis testify that the digital surface model generated by means of optical stereoscopy, based on SPOT 5 HRG images, is the most accurate; the model has a root mean square error for the Z heights of ± 3.46 m (15 m resolution). Concerning the digital surface models generated through interferometry, the best model is represented by the one created using the ERS Tandem images, with a root mean square error for the Z heights of ± 4.75 m (25 m resolution). The TSX SM model has a root mean square error for the Z heights of ± 6.60 m, while in case of the TSX HS model the root mean square error for the Z heights is ± 11.80 m. However, the TerraSAR-X models have the advantage of a better spatial resolution: 12 m for TSX SM and only 5 m for TSX SM. As expected, due to a very large time interval, the results obtained in case of ENVISAT are not so good (± 7.93 m RMSZ, 25 m resolution). Moreover, the model does not accurately represent the characteristics of the terrain and its artifacts could not be eliminated. SRTM DSM analysis in comparison with SPOT 3D reference model shows a RMSZ of ± 2.20 m.

For test area Siret, the DSM generated based on SPOT 5 HRG data presents a root mean square error for the Z heights of ± 4.27 m when compared with the SPOT 3D reference data. SPOT 5 HRG DSM was filtered in order to generate the DEM for the test area. Significant better results are obtained when using a forest mask vector layer within the process of filtering.

7. Acknowledgements

The ERS and ENVISAT data used in this study were kindly provided by the European Space Agency (ESA) under the ESA Category-1 Proposal ID 6050. The TerraSAR-X images were acquired under the German Aerospace Center (DLR) TerraSAR-X Project, Pre-launch Proposal ID LAN_0130 and SPOT data in the framework of the Centre National d'Études Spatiales (CNES) ISIS Project no 181. The BLUH software (DEMANAL and RASCOR) was kindly offered by Prof. Dr. Eng. Karsten Jacobsen, from the Institute of Photogrammetry and GeoInformation, Leibniz University Hanover, Germany.

8. References

1. *Levin, N. - Fundamentals of Remote Sensing, 1st Hydrographic Data Management Course, Imo – International Maritime Academy, Trieste, Italy; Remote Sensing Laboratory, Geography Department, Tel Aviv University, Israel, 1999;*
2. *Jacobsen, K. - DEM Generation from Satellite Data, online athttp://www.earsel.org /tutorials/Jac _03DEMGhent_red.pdf, 2003;*
3. *Fl. Zavoianu - Fotogrammetria, Publisher: "Editura Tehnica", Bucharest, 1999;*
4. *D. Massonnet, J.C. Souryis - Imaging with Synthetic Aperture Radar, CRC Press, Taylor & Francis Group, ISBN 978-0 8493-8239-0 (CRC Press), USA, 2008;*
5. *A. Ferretti, A. Monti-Guarnieri, C. Prati, F. Rocca & D. Massonnet - InSAR Principles: Guidelines for SAR Interferometry Processing and Interpretation, ESA Publications, The Netherlands, 2007;*
6. *R. Bamler - Digital Terrain Models from Radar Interferometry, Photogrammetric Week, Wichmann Verlag, Heidelberg, 1997;*
7. *Teleaga, D.; Poncos, V.; Dana, I. F.; Nedelcu, I. & Olteanu, V. G. - Urban Infrastructure Monitoring Using Spaceborne Interferometric Synthetic Aperture Radar Techniques. In Proceedings of the 1st International Conference on Space Technology, Greece, 2009.*